

Topological modeling of reconstructive phase periodic hyperbolic surfaces: the β -quartz to keatite type transition

Barbara Bieri-Gross and Reinhard Nesper*

Laboratory of Inorganic Chemistry, ETH Zurich, Wolfgang-Pauli-Strasse 10, 8093 Zurich, Switzerland

In memoriam Professor Dr. Dr. h.c. mult. Hans Georg von Schnering

Received January 21, 2011; accepted March 13, 2011

Reconstructive phase transition / Quartz / Keatite / Periodic hyperbolic surface

Abstract. The reconstructive transition β -quartz to keatite is evaluated by employing symmetry-adapted hyperbolic surfaces, *i.e.* periodic equi-surfaces (PES) as structural trial models. The PES descriptors reveal a transition model very close to the one discussed by Li et al. We can show that this model is associated with only a small shift of the principal structure factors in reciprocal space. We derive an intermediate structure halfway between quartz and keatite of $P2_1$ symmetry through symmetry considerations, and group-subgroup relations. Atomic shifts are given. It is shown that topological modeling of reconstructive phase transitions by means of periodic hyperbolic surface descriptors is a valuable extension to MD methods in exploring possible transition coordinates. As the PES-method works strictly under symmetry control along group-subgroup relations it allows for a rationalization of both global structural changes and local chemical variations. The whole transition is described by means of only one significant set of structure factors for quartz and two sets for keatite.

1. Introduction

The use of Hyperbolic Periodic Surfaces (PES) as a means of describing the topology of crystalline frameworks already goes back a while. About 30 years ago, Andersson [1] started to describe crystal structures by the help of periodic minimal surfaces (PMSs). This concept was cast into a much more practical and powerful tool by deriving topologically equivalent Periodic zero Potential (POPS) [2] and finally Periodic Nodal Surfaces (PNSs) as structure descriptors [3]. Since then, much work has been invested in correlating such bicontinuous, curved hyperbolic PMSs, POPSs, and PNSs to general crystal chemistry.

These efforts have been concerned with the elucidation of the organization of chemical bonding in three-dimensional space and, with the understanding of general principles of structure formation [1, 3–7] even reconstructive phase transitions were approached in a novel way [6, 8]. Just recently, an old prediction based on POPS analysis [2] was confirmed by state of the art quantum mechanical calculations [9].

2. Method

The most effective method for the generation of periodic hyperbolic surfaces is provided by short Fourier series under strict symmetry control [3]. This paves a straightforward way to define the simplest topological descriptor of the general topology of a space group [8] and a consecutive series of more and more complicated ones by the systematic addition of SF sets with increasingly higher moduli (reciprocal Miller indices hkl resp. longer \mathbf{k} vectors). Any such summation is characteristic for a specific space group, dependent on

- the set of equivalent reciprocal vectors and the permutation of their phases as well as
- the way of combining different sets of structure factors.

The latter means that individual SF sets, say SF_a and SF_b , may be defined such as to belong to the same or to different symmetry groups. In the latter case, the resulting surface shows the symmetry of a common subgroup and the group-subgroup relations can be worked out in a rigorous and elegant way. Explicitly,

$$\sum_h \sum_k \sum_l |S(hkl)| \cos [2\pi(hx + ky + lz) - \alpha(hkl)] = 0 \quad (1)$$

defines a periodic nodal surface (PNS) and the non-zero cases,

$$\sum_h \sum_k \sum_l |S(hkl)| \cos [2\pi(hx + ky + lz) - \alpha(hkl)] = \text{const.} \quad (2)$$

* Correspondence author (e-mail: nesper@inorg.chem.ethz.ch)

denote periodic equi-surfaces. PES are of lower symmetry than the parent PNS provided that the two tunnel systems on both sides are congruent [3].

For each reconstructive phase transition (RPT) between two limiting structures consisting of N particles there are $3N-6$ degrees of freedom in configurational space. Thus, for a mole of matter in principle there is a huge number of transition possibilities. It is quite reasonable to assume that most of them do not come into play because they either involve too much activation energy or too long diffusion pathways to compete with a small number of transitions fulfilling both requirements: low activation barrier and short diffusive if not just only displacive movements of the basic structural units. Contrary to most approaches in this research field we start from the basic idea to model RPTs by the help of PNS and PES with respect to shortest diffusive or displacive movements and not by energy minimization. Furthermore, we do not scan configurational space freely but in a most focused way such that we utilize pre-existing information, namely the notion of the limiting crystal structures of a phase transition. This is achieved by applying a Fourier decomposition to the topological problem such that

1. we use as much topological information as possible. Thus we try to **link the limiting structures** (which are known) through a topological pathway which is as simple and short as possible¹.
2. the limiting structures are represented by **envelope functions** which arise from Eqs. (1) or (2) by sets of SFs which are as small as and as close as possible to the origin of reciprocal space to furnish for the simplicity requirement.
3. the **topological pathway** is represented by systematic deformations of the structure envelopes between the limiting structural cases such that there is never a complete disruption of the envelope function into unconnected pieces. This provides means to derive continuous displacements of the unchanged building groups of the structures, in general (but not necessarily) the atoms, from structure A to B, respectively. It is understood that the resolutions defined by the SF sets have to be chosen such that these building groups are resolved to a reasonable extent.

The choice of the mutual orientations of the limiting structures is the crucial step of the topological definition of the transition pathway. As there is a huge number of possible pathways there is also a similarly large number of possible orientational correlations. A sensible choice of mutual orientations according to the criteria given in [10] leads to the definition of a Common Unit Cell (CUC) for both limiting structures. This CUC constitutes the spatial environment for the following PES investigation. A novel approach to the problem of defining a CUC based on mappings of structure factors in reciprocal space is briefly sketched further downwards, and outlined in more detail in [10].

For the present work we use the commercially available "Advanced Visualization System" (AVS, [11]) to-

gether with two extra module packages that allow for the display and investigation of chemical structures (STM3, [12]) and Periodic Equi Surfaces (CURVIS, [13]).

3. The silicon dioxide phase system

Silicon dioxide is one of nature's most abundant minerals, and at least a dozen polymorphs of pure SiO_2 have been recorded to date [14]. The low-pressure crystalline modifications consist of networks of corner-sharing SiO_4 tetrahedra, while at elevated pressures Si is also encountered in octahedral coordination [15].

First PES examinations of the lower pressure silicon dioxide phases (quartz, tridymite, and cristobalite) and of phase transitions between them have been performed by Leoni and Nesper [6, 8], whereas the high pressure modifications, keatite and coesite, have not been covered by this method up to now.

Experimental studies on the phase transition from the β -quartz to the keatite structure type for silicon dioxide are scarce and not very detailed. This is probably at least partly due to the fact, that keatite is not a naturally occurring polymorph of silicon dioxide, and that the growth of single crystals of other than microcrystalline dimensions seems to be challenging [16]. Paul P. Keat, who first synthesized the keatite phase of SiO_2 [16], only briefly mentions its successful transformation to the lower pressure modifications under the conditions matching the thermodynamic range of stability of the respective low pressure phase. Bettermann and Liebau [17] give qualitative pressure and temperature ranges for the keatite synthesis and consecutive transformation to β -quartz, as well as some kinetic estimates, but again only in the context of the hydrothermal synthesis route. It remains therefore unclear whether the direct solid-solid transformation from β -quartz to keatite does really occur in pure SiO_2 , and if so, one may ask what its characteristics are.

For the case of so-called "stuffed derivatives" of keatite and quartz with $\text{LiAlSi}_2\text{O}_6$ composition, this transition has been subject to a prior investigation by Li [18], and we chose his structural data for the two polymorphs of $\text{LiAlSi}_2\text{O}_6$ [19, 20] as well as his supercell choice and atom numbering scheme introduced in [18] in order to be able to compare our results to Li's work. However, we introduced an important simplification: Since the main interest, in the context of the phase transition lies on the transformation of the tetrahedral framework, we are not primarily interested in the lithium positions. In addition, at temperatures where the framework reorganizes, lithium is supposed to be very mobile anyhow. For these reasons, Li was omitted and Al/Si positions with mixed occupation in the framework were taken as a common building center denoted by Si only. A comparison of the structural data of keatite [21] and of $\text{LiAlSi}_2\text{O}_6$ [20] shows that the tetrahedral frameworks in both compounds are indeed practically identical.

In the following sections, the PES approach is applied to the reconstructive transition between the β -quartz and the keatite structure types. We define PES representatives for both limiting structures and determine a transition

¹ A. Einstein in R. Sessions, *New York Times* (8 January 1950): "Make everything as simple as possible, but not simpler."

pathway by linear interpolation. Furthermore, we investigate and characterize a distinct intermediate structure along our proposed transition path.

4. Cell choices

The β -quartz structure is stable above 573 °C at ambient pressure and consists of interlinked helical chains of vertex sharing SiO_4 tetrahedra. The linkage of the chains leads to the formation of 6- and 8-membered rings of tetrahedra. Depending on the handedness of the helices, the space group of β -quartz can either be $P6_422$ or $P6_222$, Si and O occupying Wyckoff sites 3c and 6j. The hexagonal standard unit cell contains three SiO_2 units.

In contrast to the quartz modifications, the keatite form consists of 5-, 7-, and 8-membered rings of tetrahedra, which involves considerable changes in topology for a phase transition between the two phases. Keatite crystallizes in space group $P4_32_12$, where silicon is partly on Wyckoff site 4a, and partly in the general position 8b. Oxygen atoms occupy three different 8b sites. One keatite unit cell thus contains twelve SiO_2 units and twelve SiO_4 tetrahedra.

As the tetragonal keatite unit cell has four times as many SiO_2 units as the hexagonal quartz cell, the latter has to be enlarged by a factor of four in order to match the total number of atoms involved in the transition. Although it converts a right-handed to a left-handed coordinate system, we chose the matrix \mathbf{n}^{-1} given in [18] as transformation matrix \mathbf{P}_1 , in order to obtain atom positions comparable to the ones of Li:

$$\mathbf{P}_1 = \begin{pmatrix} 1 & 1 & 1 \\ 1 & 1 & -1 \\ 1 & -1 & 0 \end{pmatrix}$$

In case of the chiral space group $P6_222$, the conversion from a right-handed to a left-handed coordinate system equals to the transition to the enantiomorphic space group, $P6_422$. Of course left-handed as well as right-handed crystals exist for quartz and it is trivial to mention that this conversion does not cause any substantial difference for the PES investigation of the phase transition to the keatite type.

However, the origin shift of $(1/4, 1/4, 1/6)$ given by Li has to be applied before the lattice transformation in space group $P6_422$ in order to match the cell setting and atom coordinates given in [18]. The result of this transformation is a monoclinic cell in nonstandard setting with $a = b = 7.555 \text{ \AA}$, $c = 9.036 \text{ \AA}$, $\alpha = \beta = 90^\circ$ and $\gamma = 92.65^\circ$. The tetragonal keatite cell can be maintained in its standard setting. The cell parameters are indeed very close to those of the transformed quartz cell: with 7.541 \AA the keatite a axis is only about 1.4% shorter and its c axis with 9.156 \AA about 1.3% longer than those of quartz. Projections along the c direction of both the keatite and the transformed quartz cells, respectively, are shown in Figure 1.

Another valid cell choice is based on the Bärnighausen tree relating the β -quartz and the keatite structure type via their highest symmetrical common subgroup, $C222_1$. This is outlined in more detail in [10].

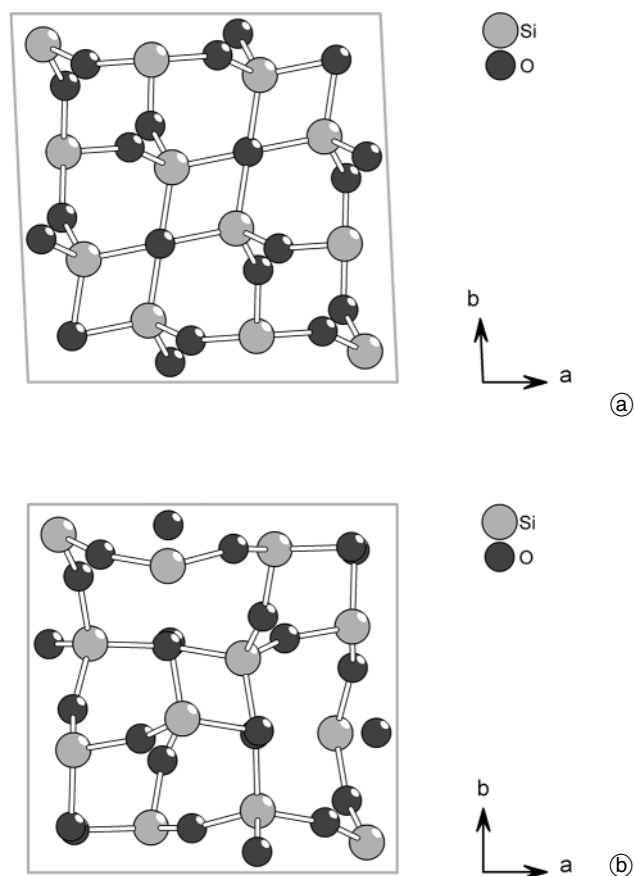


Fig. 1. Transformed quartz unit cell ((a), note the angle $\gamma = 92.65^\circ$) and keatite unit cell (b).

5. PES representatives

The PES descriptor for the β -Quartz structure type can be constructed using the strongest Bragg reflection only. In the standard setting, this is the (011) set of six equivalent reflections. For the Keatite structure, the standard setting is maintained and the PES representation is constructed from three sets of reflections. Table 1 lists the reflection sets, phase angles and weighting factors used for the construction of the PES descriptors for both structures. Figures 2 and 3 show the resulting surfaces together with the unit cells corresponding to the cell choice proposed by Li.

6. The β -quartz to keatite transition

Considerations in reciprocal space

In the tetragonal space group of keatite, $P4_32_12$, the (201) reflection set consists of four equivalents, while $(1 -1 2)$ and $(1 -1 -2)$, which are part of the hexagonal (201) set, belong in the tetragonal case to a different, independent set (c.f. Table 1). It is therefore quite obvious that the changes within these two sets of reflections mirror an important part of the structural changes during the phase transition from β -quartz to keatite. However, only by addition of the (012) set of SFs to the keatite PES, we can construct a transformation model that allows to follow the

Table 1. Reflections taken into account for the construction of the PES descriptors for the β -quartz and keatite structures, in the standard setting and in the cell setting corresponding to the work of Li [18]. Quartz structure transformed using the matrix P_1 to match the keatite (maintained) in standard setting).

β -Quartz structure hkl (standard setting)	hkl (transformed cell)	phase angle (transformed cell)	weight
011	201	$-5\pi/6$	1.0
0 1 -1	0 2 -1	$-\pi/6$	
101	2 0 -1	$-\pi/6$	
1 0 -1	021	$-5\pi/6$	
1 -1 1	1 -1 2	π	
1 -1 -1	1 -1 -2	$-\pi$	
Keatite structure hkl (standard setting, maintained)		phase angle (standard setting)	weight
021		$-3\pi/4$	1.0
0 2 -1		$-\pi/4$	
2 0 -1		$-3\pi/4$	
201		$-\pi/4$	
1 -1 2		$-\pi$	0.5
1 -1 -2		$-\pi$	
1 1 -2		0	
112		0	
0 1 -2		π	0.5
012		π	
102		π	
1 0 -2		$-\pi$	

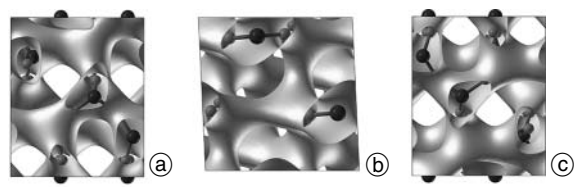


Fig. 2. PES descriptor ($q = 0.80$) for the quartz structure type (d). Projections: (a) ac plane, (b) ab plane, (c) bc plane. Large, dark spheres represent silicon, small light ones represent oxygen.

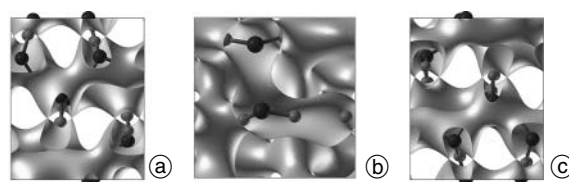


Fig. 3. PES descriptor ($q = 0.80$) for the keatite structure type (d). Projections: (a) ac plane, (b) ab plane, (c) bc plane. Large, dark spheres represent silicon, small light ones represent oxygen.

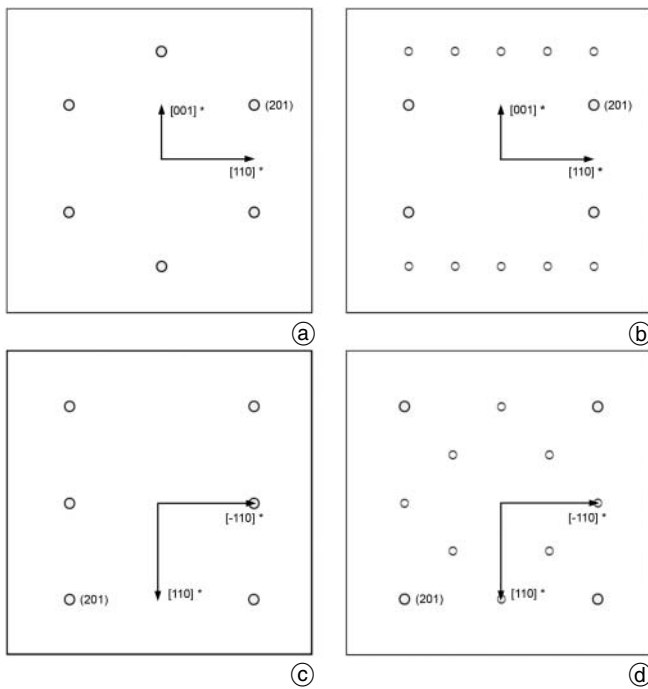


Fig. 4. Reflections taken into account for the calculation of the PES descriptors of the *b*-quartz structure (left, (a) and (c)) and of the keatite structure (right, (b) and (d)), in projection along the sixfold axis ($[1 \ -1 \ 0]^* = c^* = c$) of quartz (top, (a) and (b)) and in projection along the fourfold axis ($[001]^* = c^* = c$) of keatite (bottom, (c) and (d)). All directions given refer to reciprocal space.

migration path of individual atoms in the course of the network reorganization.

Figure 4 shows projections of the reflection sets used in the transformation model in two different directions, once along the six-fold axis of the hexagonal β -quartz structure (in the transformed cell this is the $[1 \ -1 \ 0]$ direction), and once along the four-fold axis in the tetragonal keatite structure. The radii of the circles correspond

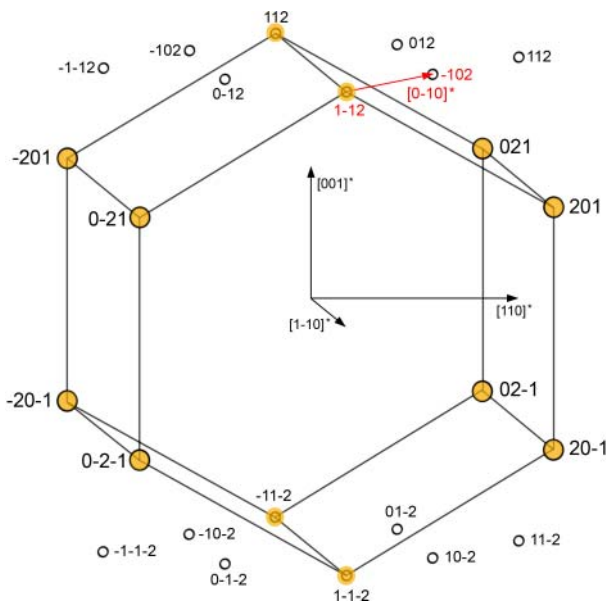


Fig. 5. Perspective view of the reflections relevant to the transition. Reflections present in quartz are marked in orange. Black open circles represent keatite reflections, different sizes correspond to different weighting factors. The red arrow designates a reciprocal analogue to the burgers vector. All directions given refer to reciprocal space.

roughly to the weighting factors. On comparison of the subfigures it becomes obvious that two reflections out of the hexagonal set of quartz split up during the transition to keatite due to the lowering of symmetry by passing through the subgroup. The direction of this splitting can be regarded as a reciprocal analogue to the burgers vector in real space. A perspective sketch of the reflections relevant to the transition is shown in Figure 5. From Figs 4 and 5 it is well seen that the additional reflections introduced for the description of the keatite type collect diffraction information of the Fourier transform of tetrahedral building units which is contained for the quartz type in just one set alone.

The PES transition model

Linear mixing of both, quartz and keatite surfaces results in a smooth surface transformation without truncations, thus enabling the derivation of intermediate atom positions and opening the possibility to develop a short transformation pathway. Different stages of transformation are shown together with a graph of the development of coordination number of silicon under the transition in Fig. 6. The increase of coordination number indicates a transition state at the silicon which has a larger coordination number than $CN=4$ as in the limiting structures. This is very well in accordance with knowledge from catalysis and from ionic mobility in solids as well as from molecular silicon chemistry. The PES descriptor opens a fifth channel (considered by the solid line in Fig. 6, bottom). However there are two more close oxygen neighbors approaching through that channel giving rise to a sixfold transition state with average Si – O distances of 2.39 Å.

Figure 7 shows the development of the intensities of the reflections and the changes of phase angles along the transformation coordinate.

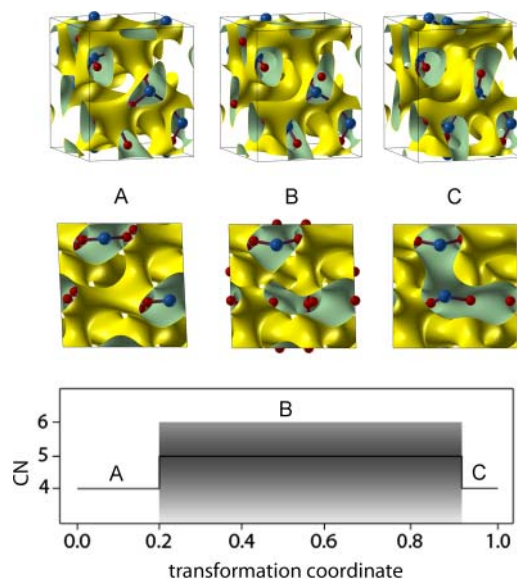


Fig. 6. Development of the coordination number of silicon during the transition at $\varrho = 0.60$. A – quartz, B – 50% transformation, C – keatite. 2nd row of pictures shows projections in *c* direction. The grey zone in the lower diagram indicates the ambiguity of assigning clearly defined coordination numbers.

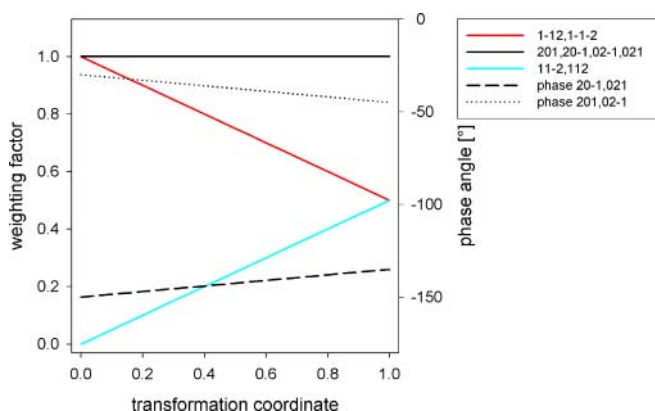


Fig. 7. Development of splitting of the Laue sets, of amplitudes and of phase angles along the transformation coordinate (0 = quartz, 1.0 = keatite).

The transition mechanism

In his work [18], Li investigates very meticulously the mechanistic possibilities in which the tetrahedral framework of the quartz structure can be transformed into that of the keatite structure. In comparison, we found our transition

model to agree well with his overall conclusion that only two out of 12 silicon atoms inside the unit cell change their bonding states and that only four out of the 48 Si–O bonds are broken. Moreover, our model apparently corresponds best to one particular case out of Li's four mechanistic propositions denoted A1, A2, B1 and B2, respectively in [18]. The rearrangement processes are investigated and compared to our work in detail in [10].

We can establish that according to our PES model, Li's A2 mechanism is closest to what we derive here. This is easily verified by adopting the numbering scheme from [18] and comparing the transformation of the surface, especially the formation of new channels and the closing of existing ones, to the bonding changes in Li's connection table. But instead of one or the other possibility out of the two degenerate ones, the PES model shows that both can happen at the same time. Table 2 lists the connectivity changes found in our transition model.

Figure 8 exhibits the rearrangement of bonds at one of the two rearrangement centers (Si22). The same process happens at the degenerate position (Si21). This is not surprising, since the two silicon atoms which take part in the rearrangement are crystallographically equivalent, meaning

Table 2. Connectivity changes within the tetrahedral framework on transition from the β -quartz to the keatite structure. Atoms involved in bond cleavages are designated in bold font.

Change of local structure and connectivity							
Si22				Si21			
Quartz	Keatite		Quartz	Keatite		Quartz	Keatite
Si22	O52	Si22	O54	Si21	O54	Si21	O52
	O48		O46		O46		O48
	O47		O47		O45		O45
	O53		O53		O51		O51
Change in connectivity only							
Si22→Si21				Si21→Si22			
Quartz	Keatite		Quartz	Keatite		Quartz	Keatite
Si12	O52	Si18	O48	Si14	O54	Si16	O46
	O32		O34		O34		O32
	O38		O38		O36		O36
	O42		O58		O44		O56
No changes in internal structure and connectivity							
Connected to Si22				Connected to Si21			
Quartz	Keatite		Quartz	Keatite		Quartz	Keatite
Si13	O53	Si17	O47	Si11	O51	Si15	O45
	O33		O31		O31		O33
	O37		O37		O35		O35
	O43		O57		O41		O55
No changes in internal structure and connectivity							
Not connected to rearrangement centers							
Quartz	Keatite		Quartz	Keatite		Quartz	Keatite
Si23	O42	Si24	O41				
	O43		O44				
	O55		O57				
	O56		O58				

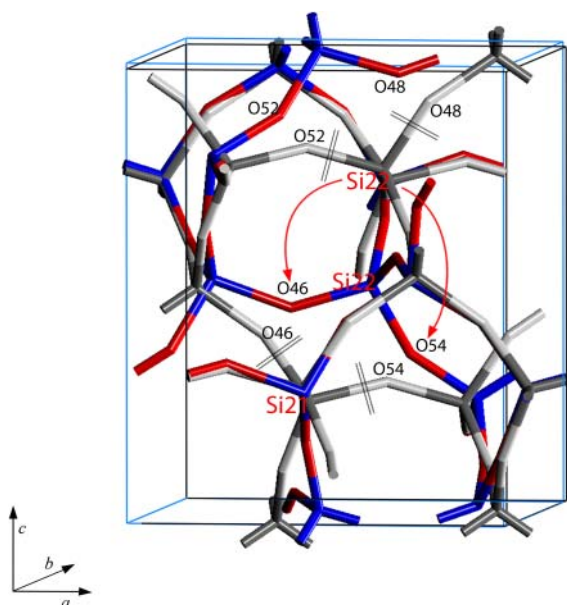


Fig. 8. Rearrangement of bonds at the Si22 rearrangement center. The keatite wireframe is shown in blue-red colors, the quartz wireframe in gray scale.

that the degeneracy would be broken only by introduction of an additional distortion with further lowering of symmetry. Of course, that can be achieved by introduction of an additional Fourier component into the transition set.

The transforming channel system envelopes both quartz and keatite during most of the transition, in fact starting from 0.3 (30%) and lasting until 0.8 on the transformation coordinate (cf. Figure 6). In that sense, the PES model implies the transformation to start with the formation of additional bonds at the transformation centers instead of cleavage of existing ones, thus revealing a transition state with higher connectivity compared to both the starting and the final structure, respectively. For keatite, being a high pressure modification of silicon dioxide, an intermediate fivefold coordination of silicon is conceivable as suggested by the PES model, even if we take into account that the pressure necessary for the formation of stishovite where silicon is coordinated octahedrally, is considerably higher (>120 kbar) than the 40 kbar applied in the hydrothermal synthesis of keatite. On the other hand, five coordinate silicon has quite frequently been encountered in metal organic chemistry these days [22].

Comparing our transition models energetically with a real bulk phase we need to make an important distinction: while we may have to consider the activation energy only for a small volume element at a time, for a bulk phase like stishovite a comparable energetic contribution would have to enter altogether into ΔH .

Considering just the connectivity of the tetrahedra instead of the rings built thereof can help to shed additional light on the framework transformation process. Table 2 reveals that we can distinguish between four types of tetrahedra according to their behavior in the course of the transition. The first group consists of the tetrahedra centered at the rearrangement centers, Si21 and Si22, and is characterized by the fact that the tetrahedra not only change their connectivity but first and foremost their internal configuration: Si21 and Si22 exchange two out of their four oxygen

neighbors in the course of the transformation. All of the other tetrahedra retain their internal geometry, but either undergo a change in connectivity with respect to their neighboring tetrahedra, or not, which divides them into two additional groups.

The last distinction can be made within the group that does neither change internal structure nor connectivity: Some of these tetrahedra are directly connected to the rearrangement centers Si21 or Si22, whilst others are not. From this point of view we see immediately that indeed only minor bonding changes are required in order to rearrange the β -quartz framework into the keatite framework.

The intermediate structure

The migration distances calculated in [10] are between 5 and 25% longer than the respective values given by Li. Additionally, they are found to be less uniform due to the obtuse angle γ gradually transforming into a right angle in the course of the transition, a process that can affect the migration distances of atoms that are in principle symmetrically equivalent in opposite ways. The overall migration distances being still relatively small, a first approach to find the intermediate structure at a transformation stage of 50% has been made by interpolating linearly between the positions of matching atoms in the starting and final structures.

Comparison with the surface at that transformation stage (isovalue $\rho = 0.8$) reveals that while for all of the oxygen positions and most of the silicon sites linear interpolation is sufficient to yield an intermediate that fits well into the channels of the intermediate surface, the interpolated positions of the transformation centers, Si21 and Si22, are not in equally good agreement with the PES model. This suggests that the migration movements of these two silicon atoms deviate quite perceptibly from the straight-lined path connecting their respective starting and final positions. These two positions can be adapted in a stepwise manner in order to represent the intermediate according to the transition model based on the channel sys-

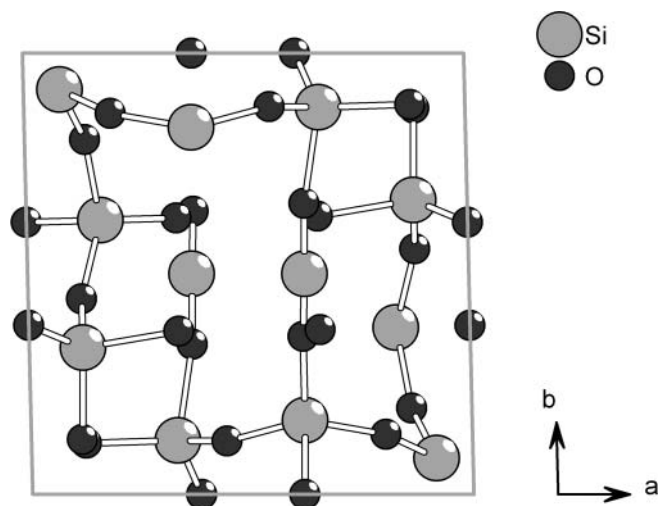


Fig. 9. Proposed intermediate structure with $P2_1$ symmetry, projection along c .

Table 3. Structural data of the proposed intermediate structure at 50% transition.

Space Group: $P2_1$			
$a = 7.548 \text{ \AA}$	$c = 9.096 \text{ \AA}$	$\alpha = \beta = 90^\circ$	$\gamma = 91.32$
Atom positions:			
Si 11	0.332	0.122	0.238
Si 12	0.122	0.332	0.762
Si 15	0.378	0.832	0.988
Si 16	0.168	0.622	0.512
Si 21	0.372	0.500	0.125
Si 23	0.082	0.918	0.750
O 31	0.443	0.121	0.393
O 32	0.121	0.443	0.607
O 35	0.383	0.000	0.125
O 36	0.000	0.617	0.375
O 41	0.125	0.116	0.299
O 44	0.884	0.876	0.201
O 45	0.379	0.642	0.063
O 46	0.540	0.627	0.424
O 51	0.369	0.340	0.176
O 52	0.340	0.396	0.824
O 55	0.195	0.864	0.896
O 56	0.136	0.804	0.604

tem of the intermediate surface. Then the resulting structure has $P2_1$ symmetry and to our knowledge does not correspond to any presently known structure type. It is shown in a projection along the c axis in Fig. 9. The calculated density of this hypothetical intermediate is estimated to 2.31 g/cm^3 and is thus between that of quartz and that of keatite (2.32 and 2.30 g/cm^3 , respectively). The theoretical structure data are summarized in Table 3.

The intermediate surface corresponds to a linear interpolation between the PES descriptors for the quartz and the keatite structure, meaning that not only amplitudes but also the phase angles arise from linear interpolation. The symmetry can directly be deduced from the permutations of the structure factors and the phase angles given in Table 3. The permutations and phase angles of the structure factors taken into account for the calculation of the intermediate surface meet the restrictions for the space group $C222_1$, whereas the intermediate has only $P2_1$ symmetry. The latter being a maximal subgroup of the former. As the symmetry reduction is not pronounced, the PES model does not account for it (cf. [10]).

7. Conclusion

In this paper we show that topological modeling of reconstructive phase transitions by means of periodic hyperbolic surface descriptors is a valuable extension to MD methods in exploring possible transition coordinates. The elegance of our method lies in the combination of reciprocal and real space information reduced to a reasonable simplicity in order to elucidate those transitions which show least intergral atomic displacements and keep intact as much of the structural arrangement as possible. Furthermore, the method works strictly under symmetry control along group-subgroup relations and thus offers a reasonable understanding of overall structural as well as of local chemical changes.

References

- [1] S. Andersson, S. T. Hyde, H. G. von Schnering, *Z. Kristallogr.* **1984**, *168*, 1.
- [2] H. G. von Schnering, R. Nesper, *Angew. Chem. Int. Ed.* **1987**, *26*, 1059.
- [3] H. G. von Schnering, R. Nesper, *J. Phys.* **1990**, *51*, C7383.
- [4] S. Andersson, M. Jacob, *The Nature of Mathematics and the Mathematics of Nature*. Elsevier, Amsterdam **1998**.
- [5] S. T. Hyde, Z. Blum, T. Landh, S. Lidin, B. W. Ninham, S. Andersson, K. Larsson, *The Language of Shape*. Elsevier, Amsterdam **1997**.
- [6] S. Leoni, *Applications of Periodic Surfaces for the Study of Crystal Structures, First Order Phase Transitions, Force Ordering, and Systematic Generation of Novel Structure Models*. ETH Zurich, **1998**.
- [7] U. S. Schwarz, G. Gompper, *Phys. Rev.* **1999**, *E 59*, 5528.
- [8] S. Leoni, R. Nesper, *Acta Cryst.* **2000**, *A 56*, 383.
- [9] E. Zurek, O. Jepsen, O. K. Andersen, *Inorg. Chem.* **2010**, *49*, 1384.
- [10] B. Bieri-Gross, *On Topological Modelling of Reconstructive Phase Transitions through Periodic Hyperbolic Surfaces*. ETH Zurich, **2007**.
- [11] *AVS/Express Developer Edition Reference Manual*. Advanced Visual Systems Inc. Waltham (Mass.), **1996**.
- [12] M. Valle, *Z. Kristallogr.* **2005**, *220*, 585.
- [13] S. Piatto, R. Nesper, *J. Appl. Crystallogr.* **2005**, *38*, 223.
- [14] N. N. Greenwood and A. Earnshaw, *Chemistry of the Elements*. 2nd ed. Elsevier, **1997**.
- [15] A. F. Hollemann, *Lehrbuch der Anorganischen Chemie*. 101 ed. de Gruyter, Berlin; New York **1995**.
- [16] P. P. Keat, *Science* **1954**, *120*, 328.
- [17] P. Bettermann and F. Liebau, *Fortschritte der Mineralogie*, Beiheft **1974**, *51*, 56.
- [18] C.-T. Li, *Acta Crystallogr.* **1971**, *B 27*, 1132.
- [19] C.-T. Li, *Z. Kristallogr.* **1968**, *127*, 327.
- [20] C.-T. Li, D. R. Peacor, *Z. Kristallogr. Kristallgeom. Kristallphys. Kristallchem.* **1967**, *126*, 46.
- [21] J. Shropshire, P. P. Keat, P. A. Vaughan, *Z. Kristallogr. Kristallgeom. Kristallphys. Kristallchem.* **1959**, *112*, 409.
- [22] H. Koller et al., *J. Am. Chem. Soc.* **1999**, *121*, 3368.